HHS Public Access

Author manuscript

Mol Genet Metab. Author manuscript; available in PMC 2016 December 01.

Published in final edited form as:

Mol Genet Metab. 2015 December ; 116(4): 281–288. doi:10.1016/j.ymgme.2015.10.011.

Correction of a Genetic Deficiency in Pantothenate Kinase 1 using Phosphopantothenate Replacement Therapy

Stephen P. Zano, **Caroline Pate**, **Matthew Frank**, **Charles Rock**, and **Suzanne Jackowski**

St. Jude Children's Research Hospital, Memphis, TN 38105 USA

Abstract

Coenzyme A (CoA) is a ubiquitous cofactor involved in numerous essential biochemical transformations, and along with its thioesters is a key regulator of intermediary metabolism. Pantothenate (vitamin B_5) phosphorylation by pantothenate kinase (PanK) is thought to control the rate of CoA production. Pantothenate kinase associated neurodegeneration is a hereditary disease that arises from mutations that inactivate the human *PANK2* gene. Aryl phosphoramidate phosphopantothenate derivatives were prepared to test the feasibility of using phosphopantothenate replacement therapy to bypass the genetic deficiency in the *Pank1*$^{-/-}$ mouse model. The efficacies of candidate compounds were first compared by measuring the ability to increase CoA levels in *Pank1*$^{-/-}$ mouse embryo fibroblasts. Administration of selected candidate compounds to *Pank1*$^{-/-}$ mice corrected their deficiency in hepatic CoA. The PanK bypass was confirmed by the incorporation of intact phosphopantothenate into CoA using tripleisotopically labeled compound. These results provide strong support for PanK as a master regulator of intracellular CoA and illustrate the feasibility of employing PanK bypass therapy to restore CoA levels in genetically deficient mice.

Keywords

PKAN; pantothenic acid; pantothenate kinase; coenzyme A

1. Introduction

Coenzyme A (CoA) is an essential cofactor that plays a central role in intermediary metabolism in all organisms. It functions as a carboxylic acid substrate carrier and supports a multitude of essential biochemical transformations, including the activities of the citric acid cycle, sterol biosynthesis, amino acid metabolism, and the synthesis and degradation of fatty acids and complex lipids [1]. CoA is synthesized in a five-step process from pantothenic acid (Pan), cysteine and ATP (Fig. 1). Pan is also known as vitamin B_5, and mammals must obtain Pan from their diet and/or intestinal flora [1]. The first committed and key regulatory step of CoA biosynthesis is the phosphorylation of Pan to phosphopantothenate (Ppan) catalyzed by the pantothenate kinases (PanK, EC 2.7.1.33)

[1,2,3]. Ppan and other pathway intermediates are not detected in radiolabeled mouse hepatocytes [4] indicating that Ppan is rapidly converted to CoA [2,5–7]. Most bacteria, fungi and lower metazoans have one gene encoding PanK, whereas mammals have three genes that express four catalytically active isoforms: PanK1α, PanK1β, PanK2 and PanK3 [3]. The four human and mouse PanK isoforms share a homologous carboxy-terminal catalytic domain, but differ in their amino-termini which direct the isoforms to different cellular compartments [8]. All cell types studied to date express several PanK isoforms [9] providing some degree of functional redundancy. The global chemical inhibition of CoA synthesis at the PanK step in mice results in a severe phenotype that leads to death [4]. The roles of individual PanKs were explored by creating global deletions of the *Pank1*, *Pank2* and *Pank3* genes in mice [10]. *Pank1* is highly expressed in liver [9], and the *Pank1*$^{-/-}$ mice have reduced hepatic CoA content and exhibit fasting hypoglycemia and steatosis [11]. The murine *Pank2* gene is highly expressed in testes [12], and *Pank2*$^{-/-}$ mice exhibit azoospermia [13]. Unlike the human *PANK2*, the murine *Pank2* is not the most abundant isoform expressed in brain [12], and is located in the cytosol rather than the mitochondria [8]. The *Pank1/Pank2* double knockout mice have low brain CoA levels, and exhibit hind limb dragging transiently during the pre-weaning period, but die within 2 weeks after birth [10].

In humans, PANK2 is the principle isoform expressed in the brain [12], and mutations in the *PANK2* gene result in the debilitating neurologic disorder called PKAN (Pantothenate Kinase Associated Neurodegeneration, OMIM ID: 234200) [14]. PKAN is the most common form of neurologic degeneration with brain iron accumulation (NBIA), a group of clinical disorders marked by progressive abnormal involuntary movements, alterations in muscle tone, and postural disturbances. PKAN is inherited as an autosomal recessive genetic condition. Two distinct manifestations of the disease are observed: (i) classic PKAN patients have more rapid progression of symptoms within the first 10 years of life and typically do not survive past age 20, and (ii) atypical PKAN does not present symptoms until the second or third decade of life with disease progression occurring much slower than the classic PKAN [15]. Several *PANK2* mutations result in a frame shift or premature stop codon in the coding sequence, and these proteins are predicted to be inactive because of the loss of the core catalytic domain sequence and are associated with early onset disease [16]. CoA synthase catalyzes the last two steps in the CoA biosynthetic pathway and NBIA patients with mutations in the *COASY* gene were recently identified [17]. Thus, disease pathogenesis is hypothesized to result from insufficient cellular CoA due to reduction of its biosynthesis. The mechanistic connections between CoA deficiency, neurodegeneration and iron accumulation in the brain are not understood. The *Pank2*$^{-/-}$ mice do not exhibit brain iron accumulation or a phenotype resembling the movement disorder that is characteristic of human PKAN patients [13].

The goal of this project was to determine if PanK bypass therapy is a viable approach to correct CoA levels in CoA-deficient animals. The rationale for this approach is based on prior research that strongly supports PanK as the rate-controlling step in cellular CoA biosynthesis [1,7]. If this is correct, all intracellular Ppan will be efficiently and completely converted to CoA. However, if PanK is not the sole regulatory point in the pathway or if

CoA degradation via nudix hydrolases plays a determinant role [18–20], then bypassing PanK may not have the desired impact on elevating CoA levels. Phosphorylated metabolic intermediates such as Ppan cannot be delivered to cells without chemical modification due to their instability in systemic circulation and limited cell membrane permeability. There have been a number of approaches developed for the protection of the phosphate moiety with substituents that are removed by intracellular enzymes [21–25]. The aryl phosphoramidate protection strategy was selected for this study because this approach has led to the development of several cell-penetrant antiviral and anticancer nucleoside analogues, and the biochemical pathway that releases the protected phosphomonoester is known [21–27]. We find that aryl phosphoramidate Ppan derivatives increase intracellular CoA levels in *Pank1*$^{-/-}$ mouse embryo fibroblasts and restore hepatic CoA levels in genetically deficient *Pank1*$^{-/-}$ mice. These results verify the key regulatory role of PanK in CoA homeostasis and show that Ppan bypass therapy is feasible.

2. Experimental procedures

2.1. Ppan derivatives

Compounds were synthesized and supplied by Retrophin, Inc. The details of chemical syntheses and compound characterizations were published previously [28].

2.2. Efficacy testing in vitro

Compounds were tested for toxicity and for metabolic conversion to CoA following addition to cultured mouse primary fibroblasts. Fibroblasts were isolated from E12.5 *Pank1*$^{-/-}$ (KO) and *Pank1*$^{+/+}$ (WT) embryos and cultured at 37°C in an atmosphere of 5% CO_2, 95% air in Dulbecco's Modified Eagle's Medium (DMEM) supplemented with 10% fetal bovine serum (Hyclone), glutamine (2 mM), penicillin (50 units/mL), streptomycin (50 μg/mL) and β-mercaptoethanol (55 μM). Compounds dissolved in vehicle were added to triplicate cultures of fibroblasts at 200 μM final concentration followed by incubation at 37°C for 24 hr. Vehicle alone (≤0.4% dimethylsulfoxide) was added to untreated control cultures. Liquid media were removed from cultures, and adherent cells (densities ranging from 3×10^6 to 9×10^6 per 150-mm dish) were washed once with phosphate-buffered saline (PBS) pH 7.4 and prepared either for quantification of CoA or determination of total viable cell number. Adherent cells in duplicate cultures were washed once briefly with ice-cold (4°C) water and immediately processed for extraction, derivatization and CoA quantification by high-pressure liquid chromatography (HPLC) as discussed below. For determination of viable cell counts, cells were detached from the dish using [0.25% trypsin + ethylene diamine tetraacetic acid] (Hyclone) and incubated for 10 min at room temperature. The action of trypsin was stopped by the addition of equal volume of DMEM containing 10% fetal bovine serum. Cells in suspension (total and viable numbers) were quantified in a NucleoCounter (New Brunswick Scientific) in buffers supplied by the instrument manufacturer. Toxicity was indicated by viability ≤ 80% or total cell number ≤ 50% compared to vechicle only-treated control cultures. Toxic compounds were not advanced to *in vivo* testing.

2.3. Efficacy testing in vivo

All animal procedures were performed according to protocols approved by the St. Jude Children's Research Hospital Institutional Animal Care and Use Committee. Derivation of the *Pank1*$^{-/-}$ (KO) mouse model was previously described [11]. Wild type *Pank1*$^{+/+}$ and KO mice were maintained on the same genetic background (strain 129SvJ × C57BL/6J). Animals were housed at room temperature 72 ± 2 °F, humidity 50% ± 10%, and a 14 hr light, 10 hr dark cycle, with the dark cycle starting at 20:00 hr. Water was supplied *ad libitum.* Animals were monitored for distress for three hours and at 24 hours after compound administration. Indicators of distress included tail twitching or stiffening, abnormal posture, loss of motor control, tremors, and/or extreme activity or lethargy. If distress was indicated, the animal was euthanized, and the compound was eliminated from further testing *in vivo*. Mice ages 8–12 weeks were used, and no significant differences in results were observed between genders.

2.3.1. Screening of candidate Ppan derivatives

Compounds were tested for toxicity in WT mice and for efficacy in KO mice. Each mouse was identified with a coded ear tag and weighed on the first day of testing. Each compound was dissolved in 75% dimethylsulfoxide and administered (5 μl/g) to 4–5 mice by intraperitoneal (IP) injection at the indicated dose and for the indicated time. Livers and brains were excised from each mouse, 20–50 mg pieces were snap-frozen in liquid nitrogen, and stored at −80 °C. For further evaluation, the lead compound was administered by IP, intravenous (IV) or oral gavage (PO) routes at a doses of 0.3, 0.6, 1.2 or 2.4 μmoles/g body weight in vehicle (PBS containing 20% (2-hydroxypropyl)-γ-cyclodextrin (HPCD), 10% dimethylsulfoxide). Untreated mice received vehicle alone. Within 7 days of the experiment, frozen liver and brain tissues were thawed on ice, weighed and analyzed for CoA content as described below. Efficacy was indicated by a statistically significant increase in the hepatic CoA level of treated mice as compared to untreated mice and by equivalence in comparison with CoA levels in untreated WT mice.

2.4.1. CoA extraction and derivatization—Fibroblasts were scraped off the culture dish, collected in 1 mL of cold water and transferred to 200 μl of 0.25 M KOH. Liver or brain tissues (20 – 50 mg) were homogenized in 2 mL of 1 mM KOH, and the pH was adjusted to 12 with 0.25 M KOH. The fibroblast cells were then incubated for 1 hr at 55°C, while the tissue homogenate was incubated at 55°C for 2 hr. The pH was adjusted to pH 8 with 1 M Tris-HCl, and CoA was derivatized with 10 μl of 100 mM monobromobimane (mBBr, Life Technologies) for 2 hr in the dark. The reaction was acidified with glacial acetic acid, and centrifuged at 500 × g for 15 min. The supernatant was added to a 2-(2-pyridyl)ethyl column (Supelco) pre-equilibrated with 1 ml of 50% methanol/2% acetic acid. The column was washed with 2 × 1 ml 50% methanol/2% acetic acid and 1 ml water. Samples were eluted with 2 × 1 ml 50 mM ammonium formate in 95% ethanol. Samples were evaporated under nitrogen and resuspended in 300 μl of water then spun through a Spin-X Centrifuge Tube Filter (0.22 μm Cellulose Acetate, Costar) to remove any precipitants.

2.4.2. CoA quantification by high-pressure liquid chromatography (HPLC)— The mBBr derivatized sample was fractionated by reverse-phase HPLC using a Gemini C_{18} 3 μm column (150 × 4.60 mm) from Phenomenex. The chromatography system was a Waters e2695 separation module with a UV/Vis detector and controlled by Empower 3 software. Solvent A was 50 mM potassium phosphate pH 4.6, and solvent B was 100% acetonitrile. Twenty microliters of sample was injected onto the column, and the flow rate was 0.5 mL/min. The HPLC program was the following: starting solvent mixture of 90% A / 10% B, 0 to 2 min isocratic with 10% B, 2 to 9 min linear gradient from 10% B to 25% B, 9 to 23 min concave gradient from 25% B to 40% B, 23 to 25 min linear gradient from 40% to 10%, and 25 to 30 min isocratic with 10% B. The detector was set at λ393 nm. The elution position of the mBBr-CoA was determined by comparison with mBBr-CoA prepared from commercial CoA (Avanti Polar Lipids or Sigma-Aldrich), and the area under the mBBr-derivatized CoA peak was integrated and compared to a range of known concentrations of the mBBr-CoA standard. The identity of the mBBr-CoA peak was confirmed by mass spectrometry (MS) after elution from the column.

2.4.3. Mass Spectrometry of CoA and mBBr-CoA—Liver was homogenized in 2 ml of methanol and 1 ml of water. After homogenizing, 1 ml of chloroform was added and incubated on ice for 15 minutes. Chloroform 1.5 ml and 1.2 ml water were added, and centrifuged at 2000 × g for 10 minutes. The top layer was loaded on a 2-(2-pyridyl)ethyl solid phase extraction column (equilibrated with 1 ml 50% methanol/2% acetic acid). The column was washed with 2 × 1 ml 50% methanol/2% acetic acid and 1 ml water. CoA and its thioesters were eluted with 2 × 1 ml of 95% ethanol + 50 mM ammonium formate, and dried under nitrogen. The samples were re-suspended in 90% methanol + 15 mM ammonium hydroxide. Mass spectrometry to determine if CoA or acetyl-CoA contained the phenyl protective group remaining on the phosphate was performed on a Finnigan TSQ Quantum (Thermo Electron, San Jose, CA) triple quadrupole mass spectrometer. The instrument was operated in positive ion SIM mode. The ion source parameters were as follows: spray voltage 4000 V, capillary temperature 250°C, capillary offset −25 V, sheath gas pressure 10, auxiliary gas pressure 0, and tube lens offset by infusion of the polytyrosine tuning and calibration in electrospray mode. The MS acquisition parameters were: scan time 0.5 s, collision energy 30 V, peak width Q1 and Q3 0.7 FWHM, Q2 CID gas 0.5 mTorr, and source CID 5 V. Neutral loss scans of 507.0 and 583.0 *m/z* were performed looking at CoA, acetyl-CoA and the derivate of each containing a possible phenyl protective group on the phosphate. Parent scan of 583.0 *m/z* was performed to determine if there was any CoA or acetyl-CoA with the phenyl protective group remaining on the phosphate.

CoA was extracted and converted to mBBr-CoA as described above. Samples were fractionated with a BEH C_{18} column (50 × 2.1 mm) attached to a Waters Acquity UPLC/ Xevo G2 quadrupole time of flight system controlled by MassLynx to determine the isotopic distribution of labeled and unlabeled mBBr-CoA. Solvent A was 50 mM ammonium bicarbonate pH 4.5, and solvent B was 100% acetonitrile. Four microliters were injected onto the column, and the flow rate was 0.75 ml/min. The elution program was: 99% A / 1% B, 0 to 0.2 min isocratic with 1% B, 0.2 to 3.5 min linear gradient from 1% B to 95% B, 3.5 to 4 min isocratic with 95% B, 4 to 4.2 min linear gradient from 95% B to 1% B, 4.2 to 5

min isocratic with 1% B. The Xevo G2 quadrupole time of flight system was operated in positive mode equipped with a LockSpray electrospray ion source. The ion source parameters were the following: source temperature 148°C, desolvation temperature 345°C, cone gas 25 L/hr, and desolvation gas 700 L/hr. The peak height for each isotope (unlabeled, $^{15}N^{13}C$-, and $^{18}O^{15}N^{13}C$-labeled) of mBBr-CoA was used to calculate the isotope distribution.

3. Results and Discussion

3.1. Candidate compounds for Ppan replacement therapy

The aryl phosphoramidate protection strategy was selected to test the feasibility of PanK bypass therapy because this approach has been validated for membrane diffusible delivery of multiple phosphorylated drugs to the cytosol and the bioactivation pathway that regenerates the free intracellular phosphate is established [21–25]. A series of 8 aryl phosphoramidate Ppan derivatives were synthesized to test the feasibility of PanK bypass therapy (Fig. 2). An α-amino acid and a phenyl moiety protected the anionic phosphate group of Ppan and the terminal carboxylic acid of Ppan was a methyl ester, except in the case of Compound 8 where the isopropyl ester was prepared. There are four steps in the aryl phosphoramide activation sequence (Fig. 3). Bioactivation of this class of prodrugs is initiated by the release of the ester protecting groups by a carboxylesterase activity. The product then undergoes intramolecular cyclization to form an unstable cyclic mixed anhydride releasing the phenol protecting group followed by the anhydride hydrolysis by water to form the phosphoramidate (Fig. 3). The monoamidate is then cleaved by an intracellular phosphoramidase to produce Ppan. The resulting Ppan would enter the CoA biosynthetic pathway downstream of PanK bypassing this key regulatory enzyme (Fig. 1). The prodrugs have chirality at the phosphorous center, but experience with other phosphate-protected compounds suggests that both diastereoisomers would be active [29].

3.2. Efficacy in mouse embryo fibroblasts

The abilities of 8 Ppan derivatives (Fig. 2) to elevate intracellular CoA were evaluated following treatment of cultured mouse embryo fibroblasts for 24 hours (Fig. 4). The *Pank1*$^{-/-}$ fibroblasts had ~50% lower CoA content compared to wild-type fibroblasts, consistent with their genetic deficiency in PanK activity (Fig. 4). The addition of Pan did not increase CoA in the fibroblasts, consistent with a key regulatory role for PanK in controlling the entry of Pan into the pathway. The inability of Ppan to increase the cellular CoA was expected due to its susceptibility to serum phosphatases and the general inability of phosphorylated molecules to diffuse across the plasma membrane. In contrast, cells treated with Compounds 1, 2, 4 and 6 showed significant increases in cellular CoA content (Fig. 4). These data indicated that the chemical substitutions on Ppan, or their metabolic derivatives, enabled transit of the compound across cell membranes and subsequent hydrolysis by intracellular hydrolases to unmask Ppan for incorporation into CoA downstream of PanK. Compounds 3, 5, 7 and 8 did not elevate CoA levels in the fibroblasts. None of the compounds showed any toxicity to the cultured cells based on cell number determinations and vital staining.

3.3. Restoration of CoA levels in Pank1$^{-/-}$ mice

The compounds that elevated CoA in the fibroblast model were evaluated in *Pank1*$^{-/-}$ mice. The *Pank1*$^{-/-}$ mice have the most marked deficiency in hepatic CoA levels following a fast [11], and so the animals were fasted overnight prior to delivery of the compounds by IP injection. Livers were removed 6 hours after treatment. Treatment with equimolar concentrations of Pan, Ppan or pantetheine (PanSH) did not result in significant differences in hepatic CoA levels between the treated and control mice (Fig. 5). Compound 2 was the most effective in elevating the liver CoA content followed by Compound 4. Compound 6, which showed an approximately 5-fold CoA increase in fibroblasts (Fig. 4), did not show appreciable CoA changes in hepatic CoA levels of *Pank1*$^{-/-}$ mice. Compound 1 has ethyl moieties at the R1 and R2 positions and did not show a significant increase in hepatic CoA. This was in contrast to the smaller methyl ester at both positions in Compound 2 which enabled significant incorporation of the unmasked Ppan to CoA. Compounds 4 and 6 with the more bulky phenyl group at the R1 or R2 positions were less effective *in vivo* than one may have predicted from the fibroblast data (Fig. 4). Mass spectrometry of the mBBr-CoA derivatives verified that the CoA from livers treated with compound 2 was indistinguishable from normal CoA and was not modified. Specifically, neutral loss scans failed to detect any CoA or acetyl-CoA that contained a phenyl group.

3.4. Compound 2 dose response in vivo

The impact of Compound 2 dose was evaluated at three different concentrations and routes of administration. Single treatments were delivered IP, intravenous (IV) or by oral gavage (PO) and livers were excised 6 hours later (Fig. 6). Compound 2 elevated hepatic CoA in all cases, although IP administration resulted in higher CoA compared to the IV and PO routes. CoA is actively metabolized in liver [11], and the ability of Compound 2 to maintain hepatic CoA levels was tested by administering a single IP dose (1.2 μmoles/g) and determining the hepatic CoA levels at 3, 6 and 12 h after treatment. Compound 2 doubled the CoA levels in the *Pank1*$^{-/-}$ livers at 3 h, but the CoA content returned to control levels at 12 h post-treatment (Fig. 7A). These data indicated that CoA turnover functions to re-establish the steady state levels within 12 h. Compound 2 administration did not significantly increase brain CoA levels (Fig. 7B), suggesting that the compound either (i) was not able to cross the blood-brain barrier, (ii) was not metabolized in the brain parenchyma, or (iii) was very low in concentration due to first-pass metabolism through the liver.

3.5 Incorporation of isotopically labeled Compound 2 into hepatic CoA

This series of experiments was performed to verify that Compound 2 bypassed PanK and the derived Ppan was incorporated into CoA. Compound 2 was synthesized with the stable isotopes ^{13}C, ^{15}N and ^{18}O incorporated into its structure (Fig. 8A). *Pank1*$^{-/-}$ mice were treated with 1.2 μmoles/g (575 mg/kg) of labeled Compound 2, and 6 h later the livers were harvested and total CoA was determined (Fig. 8B). The isotopically labeled Compound 2 was determined by quadrupole time-of-flight mass spectrometry to be 85% pure with respect to the ^{18}O-moiety. Both normal and isotopically-labeled Compound 2 increased hepatic CoA by about 50% as determined by HPLC. Mass spectrometry was then used to determine the distribution of CoA masses. Pre-existing CoA and CoA derived from dietary Pan had the

normal molecular weight and constituted about 40% of the total CoA (Fig. 8C). Also, a CoA species with a +4 mass (^{15}N, ^{13}C-CoA) was detected (Fig. 8C). This CoA species constituted 11% of total CoA and either arose from the degradation of Compound 2 to Pan followed by its subsequent incorporation into CoA by the activities of PanK2/PanK3, and/or represented a portion of the triple-labeled Compound 2 that lacked the ^{18}O-labeled phosphate moiety. The CoA species with a +6 (^{15}N, ^{13}C, ^{18}O-CoA) mass constituted 49% of the total CoA and corresponded to the incorporation of intact Ppan from Compound 2 into CoA via a PanK bypass. A representative mass spectrum of a liver sample illustrating the separation of the three isotopically distinct CoA species is shown in Fig. 8D. The correspondence between the elevation in liver CoA (Fig. 8B) and the percentage of ^{15}N, ^{13}C, ^{18}O-CoA (Fig. 8C) indicated quantitative conversion of Compound 2 into cellular CoA. These data provided direct evidence for the intracellular activation of Compound 2 to Ppan (Fig. 3) prior to its incorporation into the CoA biosynthetic pathway downstream of PanK, thus bypassing the genetic deficiency in PanK1 activity.

4. Conclusions

These results illustrate the feasibility of employing PanK bypass therapy to restore CoA levels in genetically deficient mice and provide strong support for PanK as a master regulator of intracellular CoA. The aryl phosphoramidate protected Ppan derivatives can significantly elevate intracellular CoA in PanK-deficient mammalian cells and animals. The bypass approach is possible due to the key regulatory role of PanK in the control of intracellular CoA content [7,1,11]. If there were important secondary control points in the CoA biosynthetic pathway, the elevation of intracellular Ppan would not have resulted in elevated CoA. The failure of Pan and PanSH, which both enter the pathway via PanK phosphorylation, to elevate intracellular CoA provides additional support for the stringency of PanK pathway regulation. The aryl phosphoramidate protection strategy was selected for this feasibility study because of the available background information but this approach is only one of several chemical options that could be employed for the protection and intracellular release of Ppan. These include aryloxy amino acid amidates, cyclic phosphoramidates, phosphorodiamidates, cyclic esters (*cyclo*Sal), cyclic disulfides, S-acyl-2-thioethyl phosphotriesters, pivaloyloxymethyl esters (POM), protection by attachment to lipids, and many other options [21–24,26,30–35]. An interesting alternate option may be treatment with phosphopantetheine, which rescues *Drosophila* cells deficient in CoA by bypassing PanK [36]. Each of these protection technologies have their strengths and weaknesses with respect to bioavailability and stability in mammals that will need to be evaluated to optimize the tissue penetration and plasma stability characteristics to create a Ppan prodrug with the potential to treat PKAN disease.

Acknowledgements

We thank Lois Richmond, Karen Miller and Jina Wang for expert technical assistance. We thank Retrophin Inc. for providing high purity compounds for use in this study. This work was funded in part by a Sponsored Research Agreement from Retrophin, Inc. (to S.J.), by National Institutes of Health grant GM062896 (to S.J.), and by the American Lebanese Syrian Associated Charities.

References

1. Leonardi R, Zhang Y-M, Rock CO, Jackowski S, Coenzyme A. Back in action. Prog. Lipid Res. 2005; 44:125–153. [PubMed: 15893380]
2. Jackowski S, Rock CO. Regulation of coenzyme A biosynthesis. J. Bacteriol. 1981; 148:926–932. [PubMed: 6796563]
3. Robishaw JD, Berkich DA, Neely JR. Rate-limiting step and control of coenzyme A synthesis in cardiac muscle. J. Biol. Chem. 1982; 257:10967–10972. [PubMed: 7107640]
4. Zhang YM, Chohnan S, Virga KG, Stevens RD, Ilkayeva OR, Wenner BR, Bain JR, Newgard CB, Lee RE, Rock CO, Jackowski S. Chemical knockout of pantothenate kinase reveals the metabolic and genetic program responsible for hepatic coenzyme A homeostasis. Chem. Biol. 2007; 14:291–302. [PubMed: 17379144]
5. Song W-J, Jackowski S. Cloning, sequencing, and expression of the pantothenate kinase (*coaA*) gene of *Escherichia coli* . J. Bacteriol. 1992; 174:6411–6417. [PubMed: 1328157]
6. Calder RB, Williams RSB, Ramaswamy G, Rock CO, Campbell E, Unkles SE, Kinghorn JR, Jackowski S. Cloning and characterization of a eukaryotic pantothenate kinase gene (*panK*) from *Aspergillus nidulans* . J. Biol. Chem. 1999; 274:2014–2020. [PubMed: 9890959]
7. Rock CO, Calder RB, Karim MA, Jackowski S. Pantothenate kinase regulation of the intracellular concentration of coenzyme A. J. Biol. Chem. 2000; 275:1377–1383. [PubMed: 10625688]
8. Alfonso-Pecchio A, Garcia M, Leonardi R, Jackowski S. Compartmentalization of mammalian pantothenate kinases. PLoS ONE. 2012; 7:e49509. [PubMed: 23152917]
9. Dansie LE, Reeves S, Miller K, Zano SP, Frank M, Pate C, Wang J, Jackowski S. Physiological roles of the pantothenate kinases. Biochem. Soc. Trans. 2014; 42:1033–1036. [PubMed: 25109998]
10. Garcia M, Leonardi R, Zhang YM, Rehg JE, Jackowski S. Germline deletion of pantothenate kinases 1 and 2 reveals the key roles for CoA in postnatal metabolism. PLoS. ONE. 2012; 7:e40871. [PubMed: 22815849]
11. Leonardi R, Rehg JE, Rock CO, Jackowski S. Pantothenate kinase 1 is required to support the metabolic transition from the fed to the fasted state. PLoS ONE. 2010; 5:e11107. [PubMed: 20559429]
12. Leonardi R, Zhang YM, Lykidis A, Rock CO, Jackowski S. Localization and regulation of mouse pantothenate kinase 2. FEBS Lett. 2007; 581:4639–4644. [PubMed: 17825826]
13. Kuo YM, Duncan JL, Westaway SK, Yang H, Nune G, Xu EY, Hayflick SJ, Gitschier J. Deficiency of pantothenate kinase 2 (*Pank2*) in mice leads to retinal degeneration and azoospermia. Hum. Mol. Genet. 2005; 14:49–57. [PubMed: 15525657]
14. Zhou B, Westaway SK, Levinson B, Johnson MA, Gitschier J, Hayflick SJ. A novel pantothenate kinase gene (*PANK2*) is defective in Hallervorden-Spatz syndrome. Nat. Genet. 2001; 28:345–349. [PubMed: 11479594]
15. Hayflick SJ, Westaway SK, Levinson B, Zhou B, Johnson MA, Ching KH, Gitschier J. Genetic, clinical, and radiographic delineation of Hallervorden-Spatz syndrome. N. Engl. J. Med. 2003; 348:33–40. [PubMed: 12510040]
16. Zhang Y-M, Rock CO, Jackowski S. Biochemical properties of human pantothenate kinase 2 isoforms and mutations linked to pantothenate kinase-associated neurodegeneration. J. Biol. Chem. 2006; 281:107–114. [PubMed: 16272150]
17. Dusi S, Valletta L, Haack TB, Tsuchiya Y, Venco P, Pasqualato S, Goffrini P, Tigano M, Demchenko N, Wieland T, Schwarzmayr T, Strom TM, Invernizzi F, Garavaglia B, Gregory A, Sanford L, Hamada J, Bettencourt C, Houlden H, Chiapparini L, Zorzi G, Kurian MA, Nardocci N, Prokisch H, Hayflick S, Gout I, Tiranti V. Exome sequence reveals mutations in CoA synthase as a cause of neurodegeneration with brain iron accumulation. Am. J. Hum. Genet. 2014; 94:11–22. [PubMed: 24360804]
18. Gasmi L, McLennan AG. The mouse *Nudt7* gene encodes a peroxisomal nudix hydrolase specific for coenzyme A and its derivatives. Biochem. J. 357:33–38. [PubMed: 11415433]
19. Reilly SJ, Tillander V, Ofman R, Alexson SE, Hunt MC. The nudix hydrolase 7 is an acyl-CoA diphosphatase involved in regulating peroxisomal coenzyme A homeostasis. J. Biochem. 2008; 144:655–663. [PubMed: 18799520]

20. Shumar SA, Fagone P, Alfonso-Pecchio A, Gray JT, Rehg JE, Jackowski S, Leonardi R. Induction of neuron-specific degradation of Coenzyme A models pantothenate kinase-associated neurodegeneration by reducing motor coordination in mice. PLoS ONE. 2015; 10:e0130013. [PubMed: 26052948]
21. Hecker SJ, Erion MD. Prodrugs of phosphates and phosphonates. J. Med. Chem. 2008; 51:2328–2345. [PubMed: 18237108]
22. Mehellou Y, Balzarini J, McGuigan C. Aryloxy phosphoramidate triesters: a technology for delivering monophosphorylated nucleosides and sugars into cells. ChemMedChem. 2009; 4:1779–1791. [PubMed: 19760699]
23. Mehellou Y, Valente R, Mottram H, Walsby E, Mills KI, Balzarini J, McGuigan C. Phosphoramidates of 2'-β-D-arabinouridine (AraU) as phosphate prodrugs; design, synthesis, in vitro activity and metabolism. Bioorg. Med. Chem. 2010; 18:2439–2446. [PubMed: 20299228]
24. Pradere U, Garnier-Amblard EC, Coats SJ, Amblard F, Schinazi RF. Synthesis of nucleoside phosphate and phosphonate prodrugs. Chem Rev. 2014; 114:9154–9218. [PubMed: 25144792]
25. Tan X, Chu CK, Boudinot FD. Development and optimization of anti-HIV nucleoside analogs and prodrugs: A review of their cellular pharmacology, structure-activity relationships and pharmacokinetics. Adv. Drug Deliv. Rev. 39:117–151. [PubMed: 10837771]
26. Hamon N, Slusarczyk M, Serpi M, Balzarini J, McGuigan C. Synthesis and biological evaluation of phosphoramidate prodrugs of two analogues of 2-deoxy-d-ribose-1-phosphate directed to the discovery of two carbasugars as new potential anti-HIV leads. Bioorg. Med. Chem. 2015; 23:829–838. [PubMed: 25616343]
27. Yoo CB, Valente R, Congiatu C, Gavazza F, Angel A, Siddiqui MA, Jones PA, McGuigan C, Marquez VE. Activation of p16 gene silenced by DNA methylation in cancer cells by phosphoramidate derivatives of 2'-deoxyzebularine. J. Med. Chem. 2008; 51:7593–7601. [PubMed: 19006382]
28. Vaino, A.; Biestek, M.; Shkreli, M. Pantothenate derivatives for the treatment of neurologic disorders. U.S. Patent. 8,673,883. 2014.
29. McGuigan C, Madela K, Aljarah M, Bourdin C, Arrica M, Barrett E, Jones S, Kolykhalov A, Bleiman B, Bryant KD, Ganguly B, Gorovits E, Henson G, Hunley D, Hutchins J, Muhammad J, Obikhod A, Patti J, Walters CR, Wang J, Vernachio J, Ramamurty CV, Battina SK, Chamberlain S. Phosphorodiamidates as a promising new phosphate prodrug motif for antiviral drug discovery: application to anti-HCV agents. J. Med. Chem. 2011; 54:8632–8645. [PubMed: 22039920]
30. Butora G, Qi N, Fu W, Nguyen T, Huang HC, Davies IW. Cyclic-disulfide-based prodrugs for cytosol-specific drug delivery. Angew. Chem. Int. Ed Engl. 2014; 53:14046–14050. [PubMed: 25346363]
31. Spacilova P, Naus P, Pohl R, Votruba I, Snasel J, Zabranska H, Pichova I, Ameral R, Birkus G, Cihlar T, Hocek M. CycloSal-phosphate pronucleotides of cytostatic 6-(Het)aryl-7-deazapurine ribonucleosides: Synthesis, cytostatic activity, and inhibition of adenosine kinases. ChemMedChem. 2010; 5:1386–1396. [PubMed: 20533504]
32. McGuigan C, Bourdin C, Derudas M, Hamon N, Hinsinger K, Kandil S, Madela K, Meneghesso S, Pertusati F, Serpi M, Slusarczyk M, Chamberlain S, Kolykhalov A, Vernachio J, Vanpouille C, Introini A, Margolis L, Balzarini J. Design, synthesis and biological evaluation of phosphorodiamidate prodrugs of antiviral and anticancer nucleosides. Eur. J. Med. Chem. 2013; 70:326–340. [PubMed: 24177359]
33. Meade BR, Gogoi K, Hamil AS, Palm-Apergi C, van den Berg A, Hagopian JC, Springer AD, Eguchi A, Kacsinta AD, Dowdy CF, Presente A, Lonn P, Kaulich M, Yoshioka N, Gros E, Cui XS, Dowdy SF. Efficient delivery of RNAi prodrugs containing reversible charge-neutralizing phosphotriester backbone modifications. Nat. Biotechnol. 2014; 32:1256–1261. [PubMed: 25402614]
34. Pertenbreiter F, Balzarini J, Meier C. Nucleoside mono- and diphosphate prodrugs of 2',3'-dideoxyuridine and 2',3'-dideoxy-2',3'-didehydrouridine. ChemMedChem. 2015; 10:94–106. [PubMed: 25209965]
35. Sofia MJ. Nucleotide prodrugs for the treatment of HCV infection. Adv. Pharmacol. 2013; 67:39–73. [PubMed: 23885998]

36. Srinivasan B, Baratashvili M, van der Zwaag M, Kanon B, Colombelli C, Lambrechts RA, Schaap O, Nollen EA, Podgorsek A, Kosec G, Petkovic H, Hayflick S, Tiranti V, Reijngoud DJ, Grzeschik NA, Sibon OC. Extracellular 4'-phosphopantetheine is a source for intracellular coenzyme A synthesis. Nat. Chem Biol. 2015; 11:784–792. [PubMed: 26322826]

37. McGuigan C, Thiery JC, Daverio F, Jiang WG, Davies G, Mason M. Anticancer ProTides: tuning the activity of BVDU phosphoramidates related to thymectacin. Bioorg. Med. Chem. 2005; 13:3219–3227. [PubMed: 15809157]

Highlights

- Pantothenate kinase is the first commited step in coenzyme A biosynthesis.
- Hereditary deficiency in Pantothenate kinase 2 leads to neurodegeneration called PKAN.
- Deficiency in Pantothenate Kinase 1 causes reduced coenzyme A in mouse liver.
- Phosphopantothenate replacement therapy is feasible using arylphosphoramidate prodrugs.

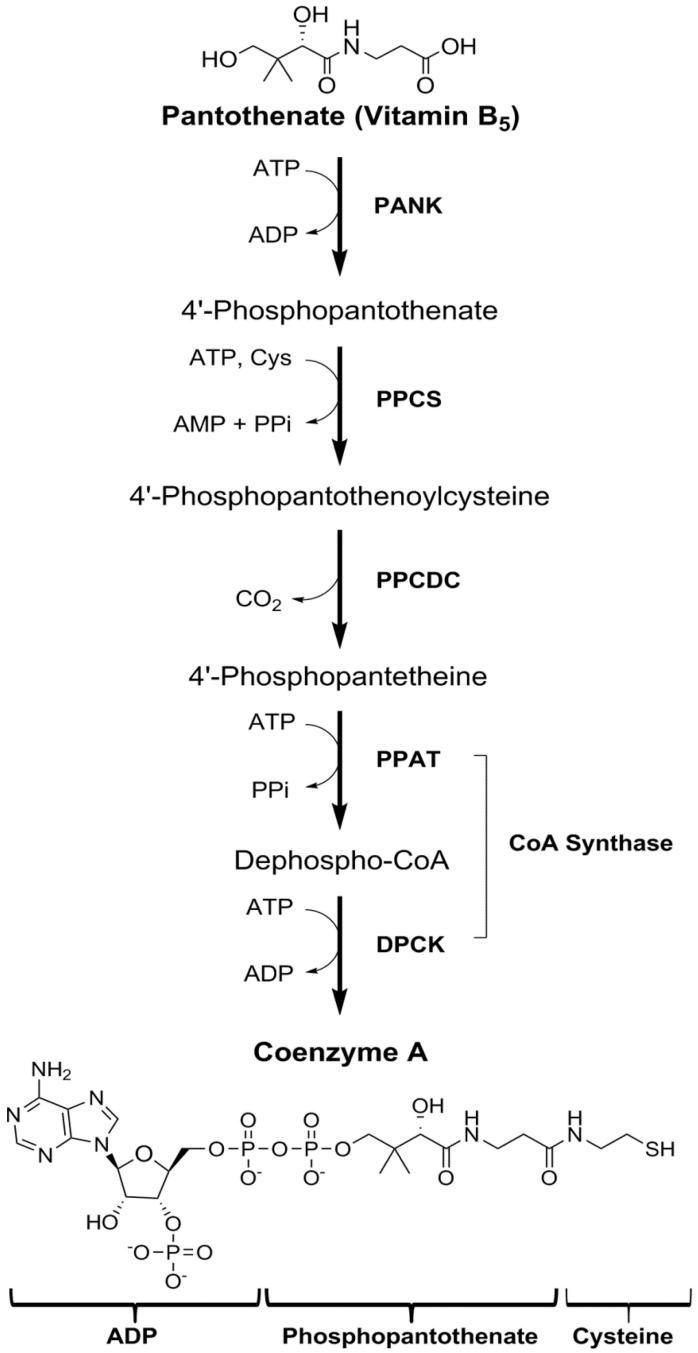

Fig. 1.

The CoA biosynthetic pathway. The commitment step is the phosphorylation of pantothenate (Vitamin B_5) by pantothenate kinase (PANK) to 4′-phosphopantothenate. This is followed by condensation with cysteine catalyzed by 4′-phosphopantothenoylcysteine synthase (PPCS) and then decarboxylation to form 4′-phosphopantetheine by 4′-phosphopanthenoylcysteine decarboxylase (PPCDC). 4′-Phosphopantetheine is adenylylated to dephospho-CoA by phosphopantetheine adenylyltransferase (PPAT), then phosphorylated by dephospho-CoA kinase (DPCK) at the 3′-OH of the ribose to form CoA.

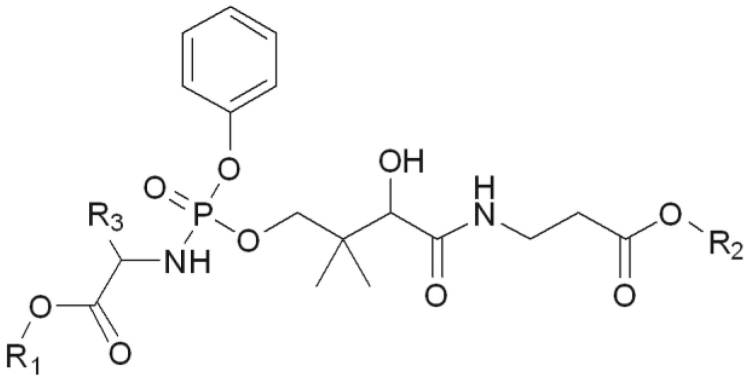

Compound	R1	R2	R3
1	Ethyl	Ethyl	Methyl
2	Methyl	Methyl	Methyl
3	*sec* Butyl	*sec* Butyl	Methyl
4	Phenyl	Ethyl	Methyl
5	Ethyl	Phenyl	Methyl
6	Phenyl	Phenyl	Methyl
7	Cyclopropyl	Cyclopropyl	Methyl
8	Ethyl	Ethyl	*iso* Propyl

Fig. 2.

Structures of aryl phosphoramidate Ppan derivatives. Eight protected Ppan derivatives with different substituents at the three indicated positions were synthesized to test their ability to bypass PanK and elevate cellular CoA.

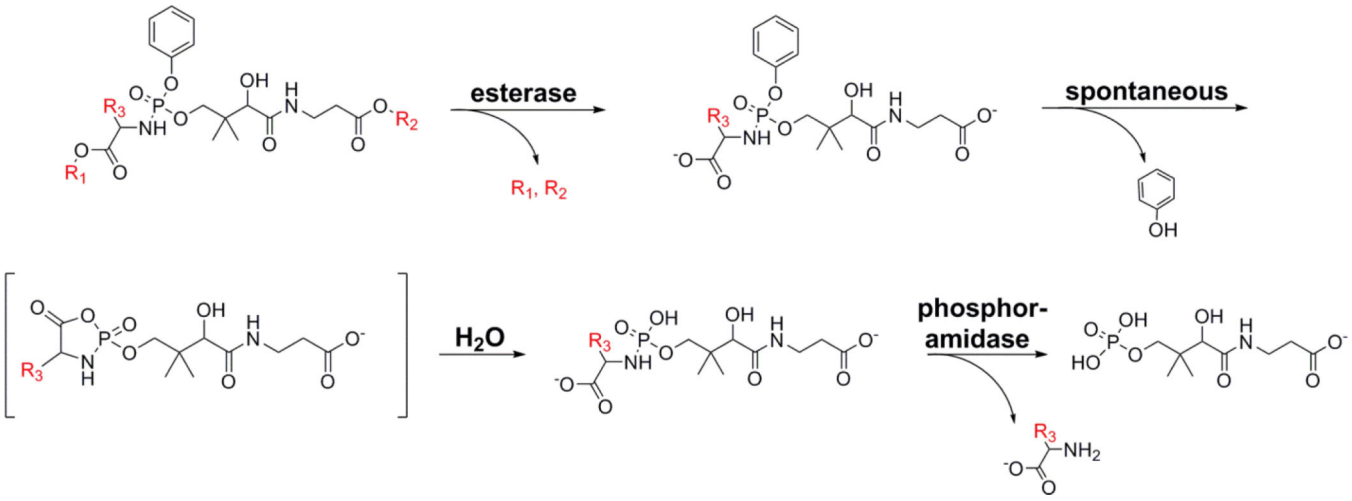

Fig. 3.

Proposed pathway for the intracellular release of Ppan from the aryl phosphoramidate protecting groups. The mechanism of activation of aryl phosorphoramidate prodrugs is established [21–25] and the scheme is adapted from [21,37]. The first step is enzymatic and occurs by the hydrolysis of either of the two esters (R1 and R2) carried out by cellular carboxylesterases. The compound then undergoes a spontaneous intramolecular rearrangement where the carboxylate attacks the phosphate forming a cyclic intermediate with concomitant release of the phenol. The unstable cyclic mixed anhydride then spontaneously hydrolyzes to the phosphoramidate. The phosphoramide (P-N) bond is then enzymatically cleaved by a cellular phosphoramidase to form Ppan. Many monophosphoramidates also spontaneously hydrolyze.

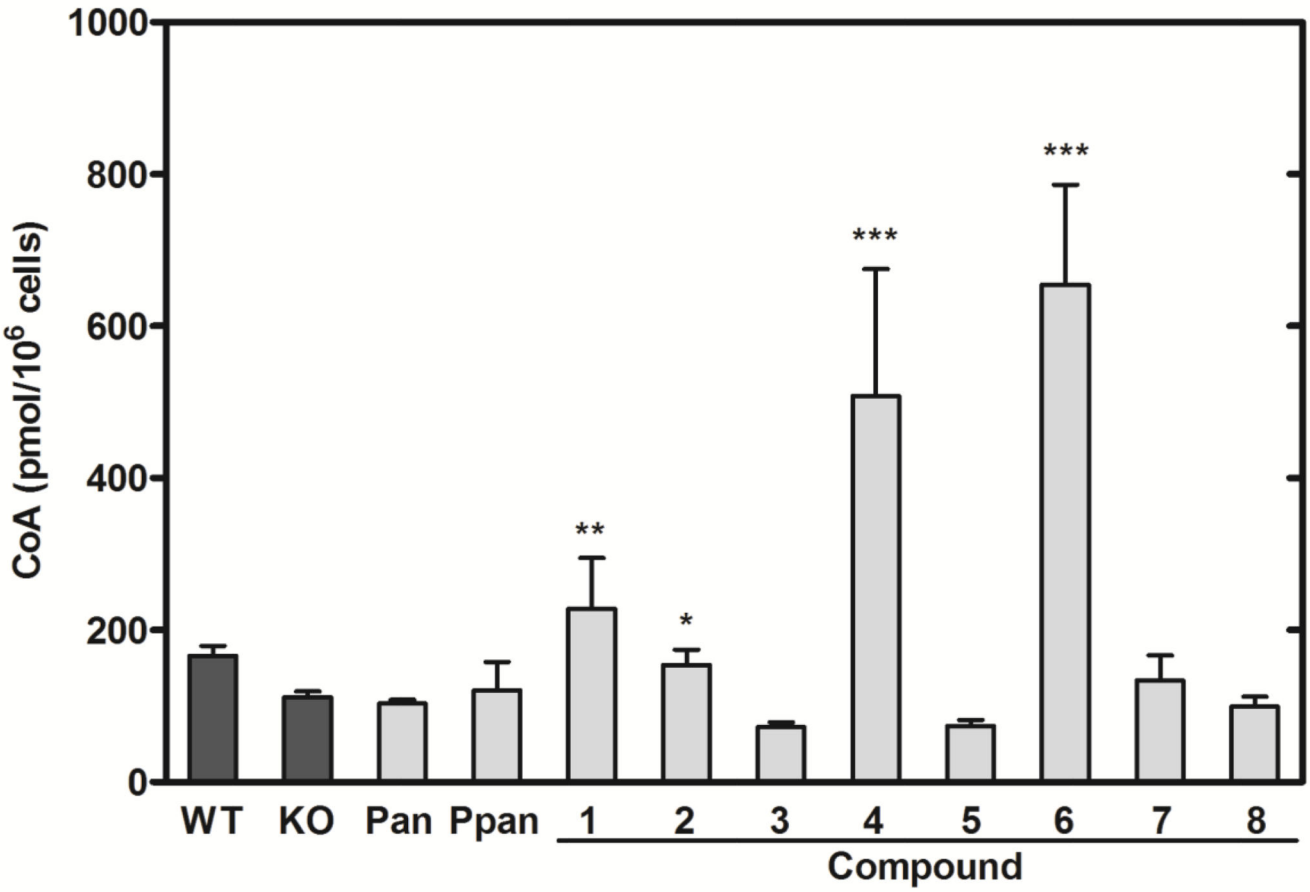

Fig. 4.

The impact of aryl phosphoramidate Ppan derivatives on the intracellular CoA content in *Pank1*$^{-/-}$ mouse embryo fibroblasts. The four control conditions were vehicle-treated wild-type fibroblasts (WT) (n=4), *Pank1*$^{-/-}$ (KO) fibroblasts (n=14) (dark bars); *Pank1*$^{-/-}$ fibroblasts treated with either 200 μM Pan (n=2) or 200 μM Ppan (n=2). *Pank1*$^{-/-}$ fibroblasts were treated with 200 μM Compounds 1–8 (n=2 per group). CoA levels (pmol/10^6 cells) were determined as described under Experimental Procedures. Significance was determined with respect to the KO values using the Student's t-test: * $p<0.05$; ** $p<0.005$; *** $p<0.0005$).

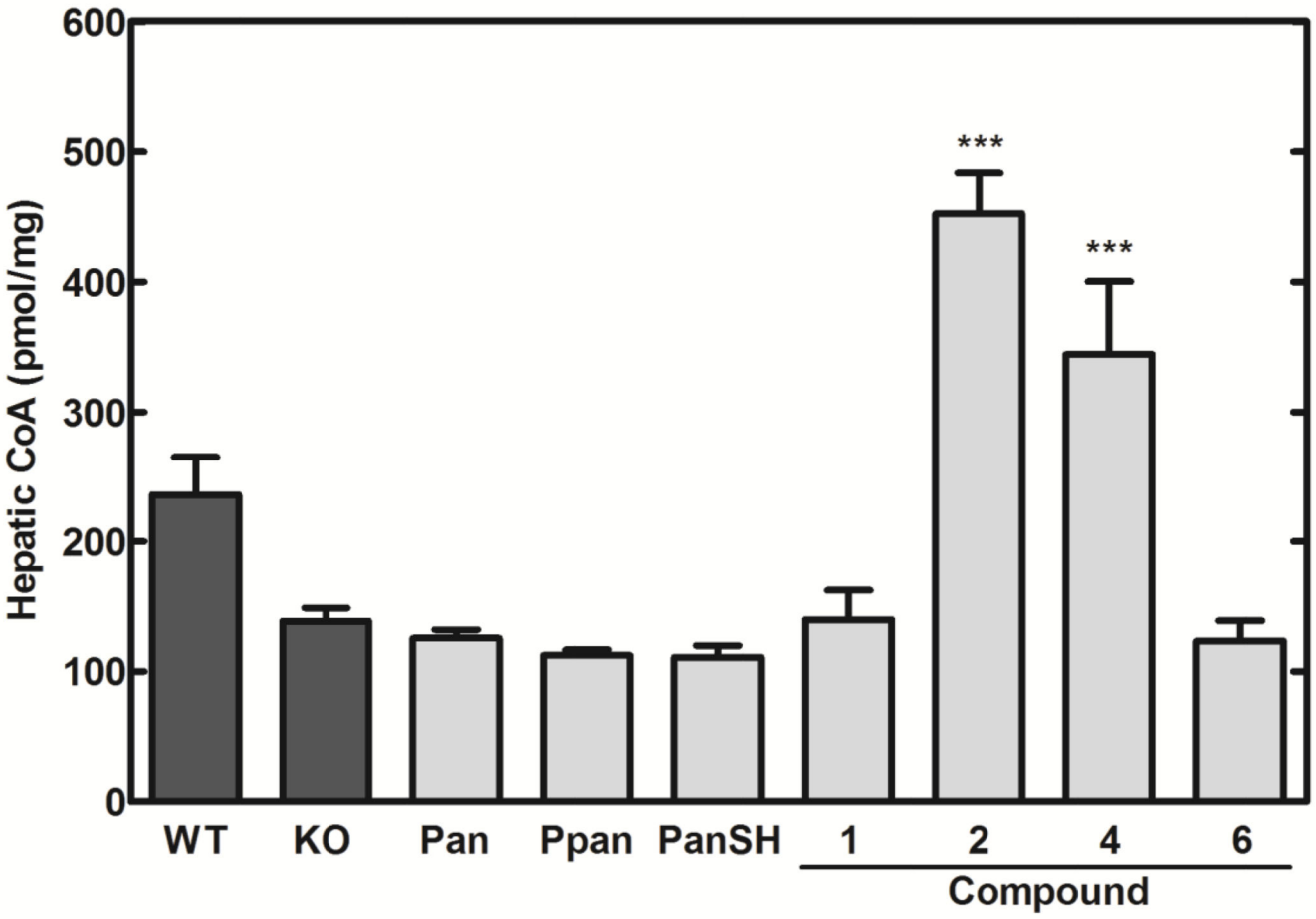

Fig. 5.

Efficacy of four selected aryl phosphoramidate Ppan derivatives in elevating hepatic CoA in the *Pank1*$^{-/-}$ mouse model. Hepatic CoA levels (pmol/mg liver) were determined for *Pank1*+/+ (WT) (n=14) and *Pank1*$^{-/-}$ (KO) (n=12) mice treated with vehicle alone (dark bars). Three control conditions consisted of *Pank1*$^{-/-}$ mice treated with 1.2 μmoles/g body weight of Pan (263 mg/kg; n=5), Ppan (359 mg/kg; n=6) or pantetheine (PanSH) (334 mg/kg; n=5). The four compounds that were positive in the fibroblast screen (Fig. 4) were tested at a dose of 1.2 μmoles/g body weight (Compound 1, 603 mg/kg; Compound 2, 569 mg/kg; Compound 4, 677 mg/kg; Compound 6, 752 mg/kg; n=9 per group, except for Compound 6 where n=2 due to limited quantities of material). Statistically significant differences with respect to KO values are presented as: * $p<0.05$; ** $p<0.005$; *** $p<0.0005$.

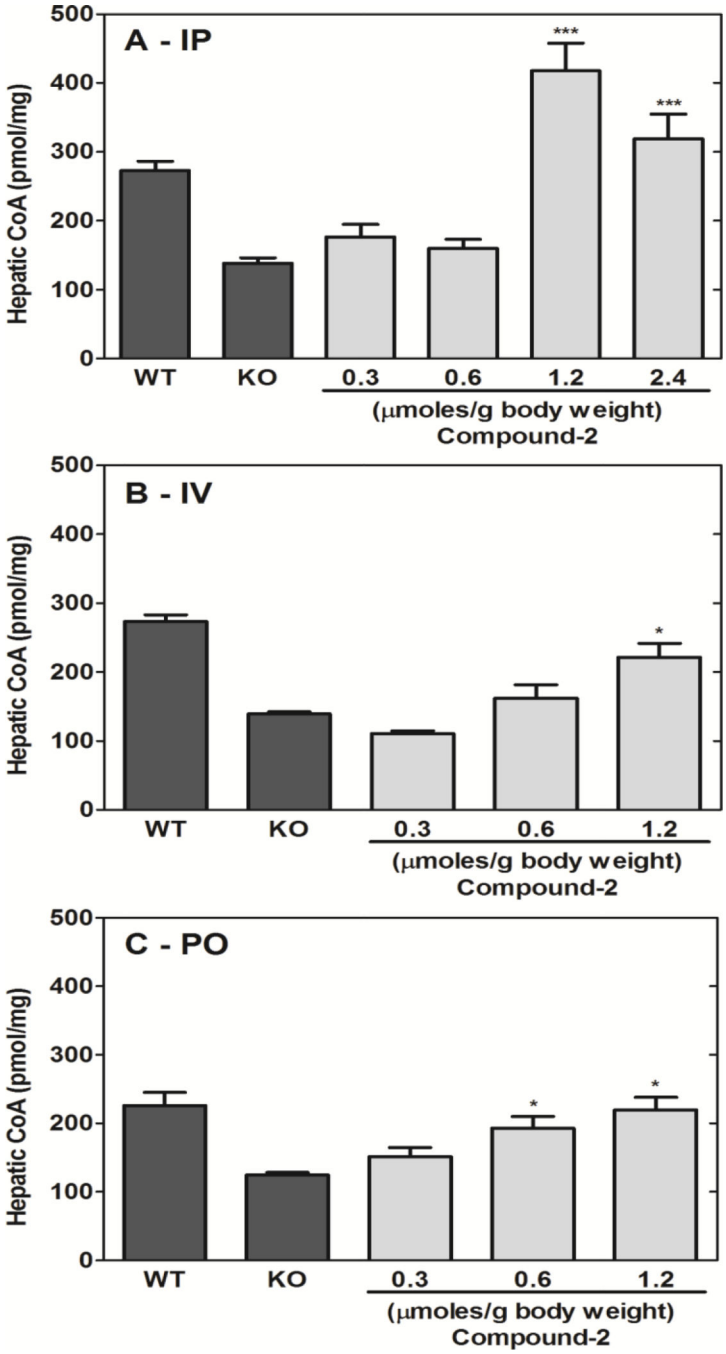

Fig. 6.

Compound 2 dose-response in *Pank1*$^{-/-}$ mice. Compound 2 was administered to mice via three routes. **A.** Intraperitoneal administration (IP). **B.** Intravenous administration (IV). **C.** Oral gavage administration (PO). *Pank1*$^{-/-}$ mice were dosed and the livers were isolated 6 hr later for CoA determinations (n = 3 per group). Statistically significant differences with respect to knockout (KO) values are presented as: * $p<0.05$; ** $p<0.005$; *** $p<0.0005$.

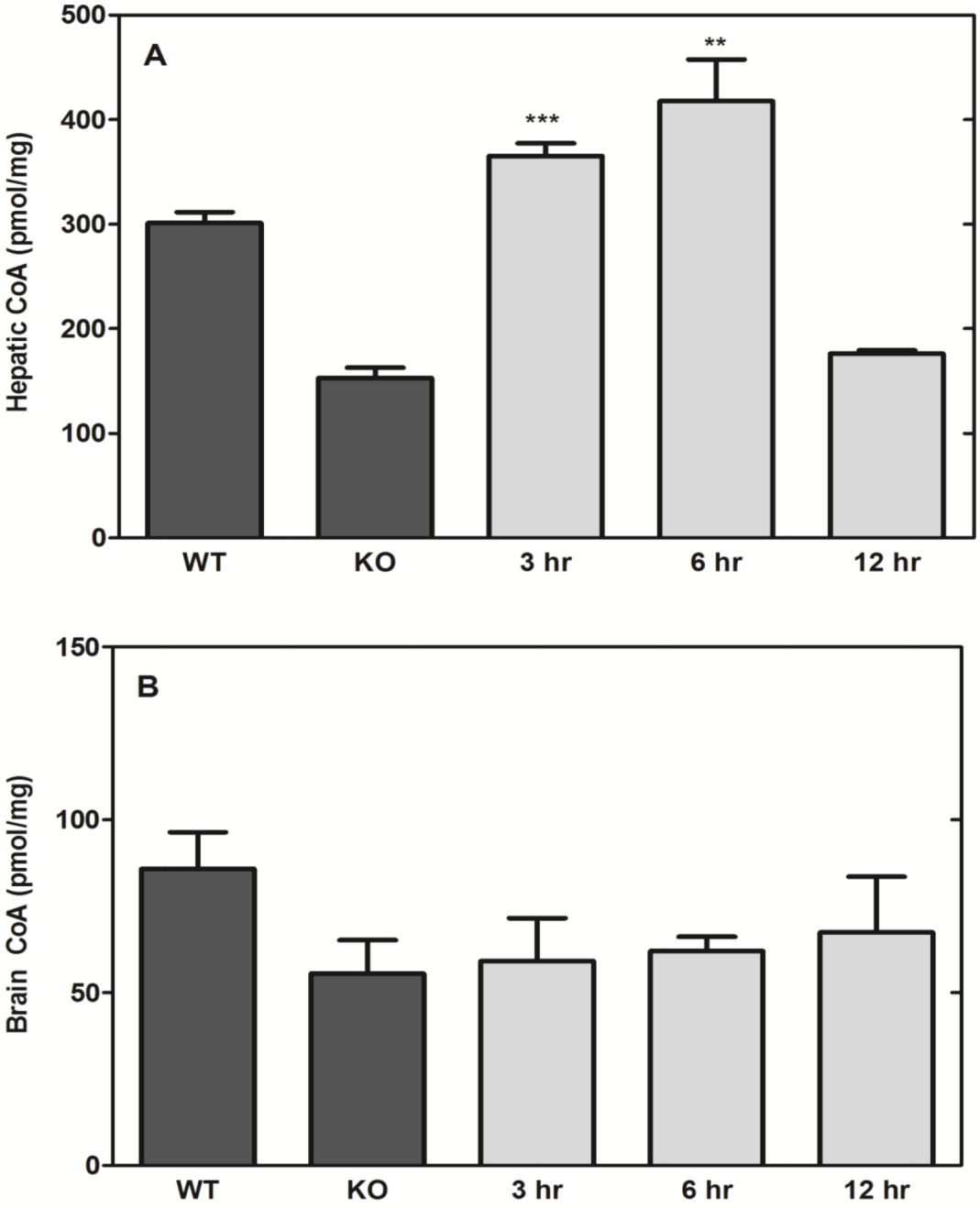

Fig. 7.

Response durability. **A.** Liver CoA. **B.** Brain CoA. Compound 2 (1.2 μmoles/g body weight; 569 mg/kg) was administered IP to *Pank1*$^{-/-}$ mice and tissues were isolated at the indicated times after treatment (n=3 per group). Statistically significant differences with respect to knockout (KO) values are presented as: * $p<0.05$; ** $p<0.005$; *** $p<0.0005$.

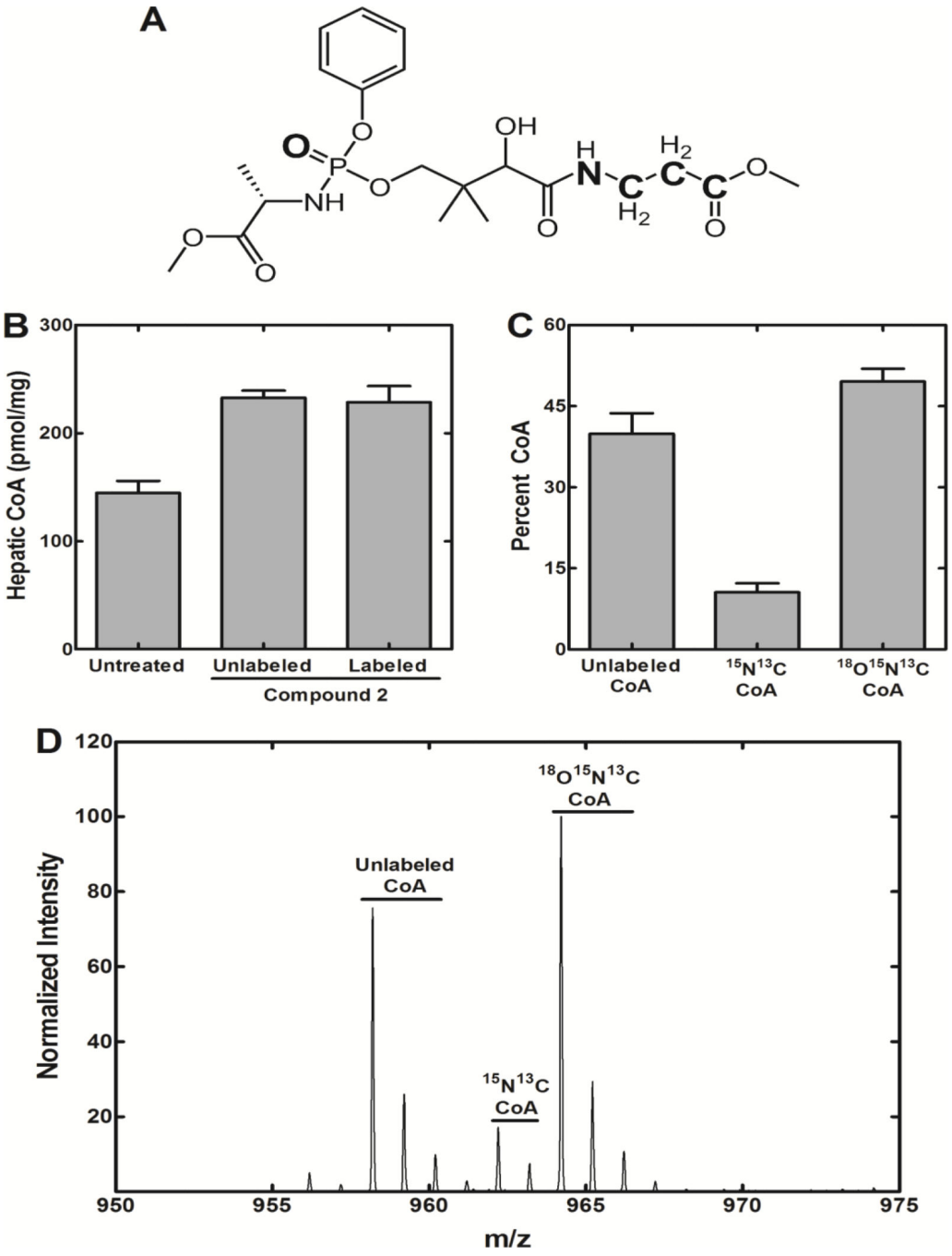

Fig. 8.

Metabolic incorporation of isotopically-labeled Compound 2. **A.** Structure of Compound 2 labeled with heavy elements (^{18}O, ^{15}N, and ^{13}C) shown in bold letters. **B.** Measurement of hepatic CoA levels in *Pank1*$^{-/-}$ mice treated with 1.2 μmoles/g either labeled or unlabeled Compound 2 (n=3 per group) for 6 hours. **C.** Isotopic distribution of hepatic CoA in mice treated with labeled Compound 2. **D.** Representative mass spectrum showing the isotopic distribution in CoA from the livers of *Pank1*$^{-/-}$ mice that were treated with isotopically labeled Compound 2. CoA with the normal mass represents pre-existing hepatic CoA prior

to labeling and the incorporation of pantothenate from the diet. ^{15}N, ^{13}C-labeled CoA (+4) represents the fraction of CoA derived from labeled Pan arising from the breakdown of the prodrug to ^{15}N, ^{13}C-labeled Pan in the circulation and its incorporation into CoA via PanK, and/or the small portion of the triple-labeled Compound 2 that lacked the ^{18}O-moiety. ^{18}O, ^{15}N, ^{13}C-labeled CoA (+6) represents the fraction of CoA derived from triple-labeled Ppan that, in turn, arose from the intracellular metabolism of the aryl phosphoramidate.